Multivariate analysis of wind stress and curl over the Japan/East Sea, based on satellite scatterometry data

O. Trusenkova

Pacific Oceanological Institute, Vladivostok, Russia

PICES 2010, October 22–31, 2010, Portland, Oregon, USA

Motivation

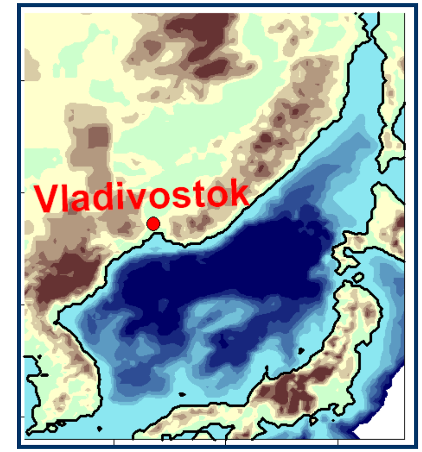

Monthly mean wind stress and curl in the JES area

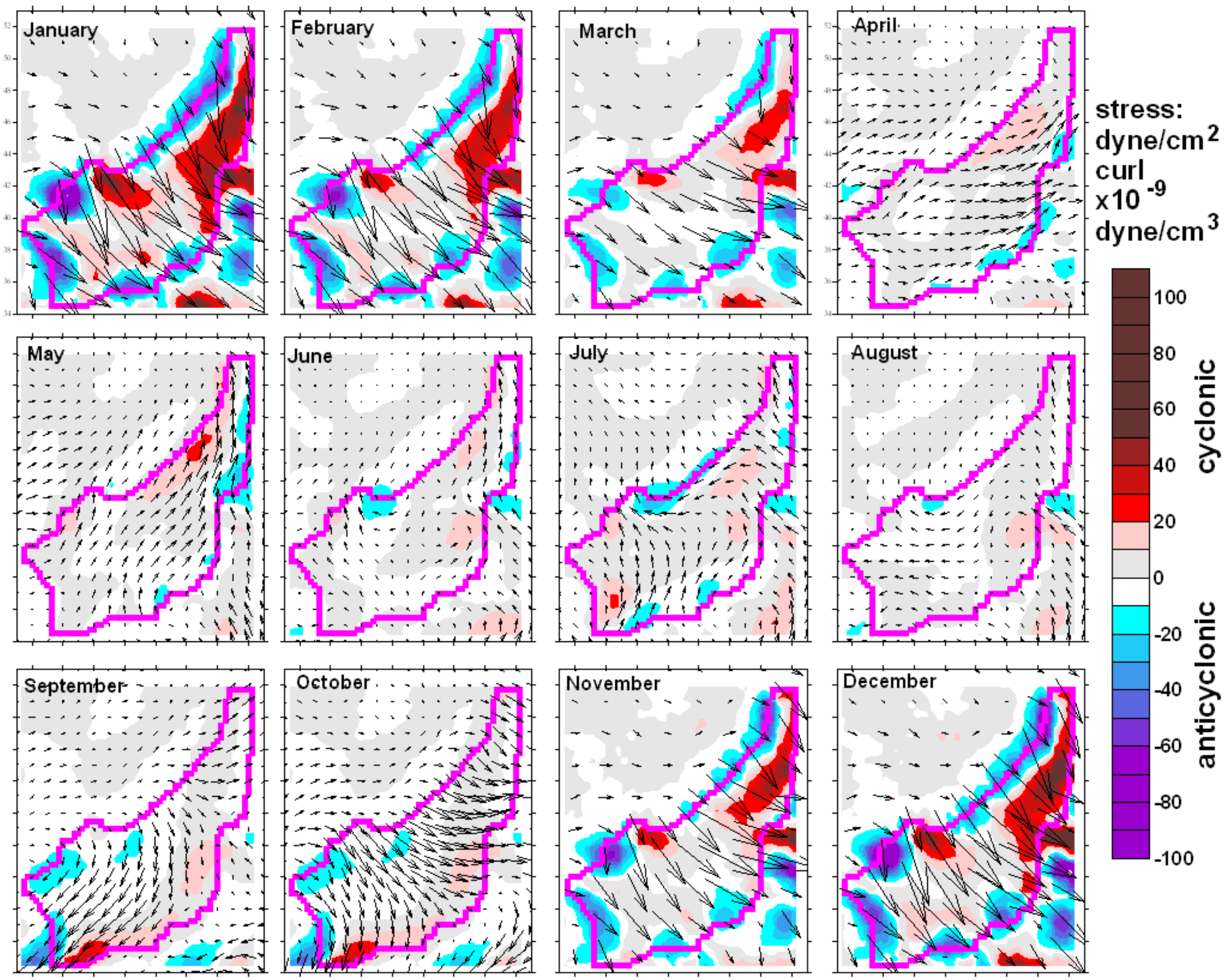

Stable conditions in winter, changeable and weak, on monthly time scale, wind in summer → Are there any patterns in summer wind?

Previous results from 1°-gridded NCEP reanalysis

(ancillary data for the SeaWifS Project)

Mode 1

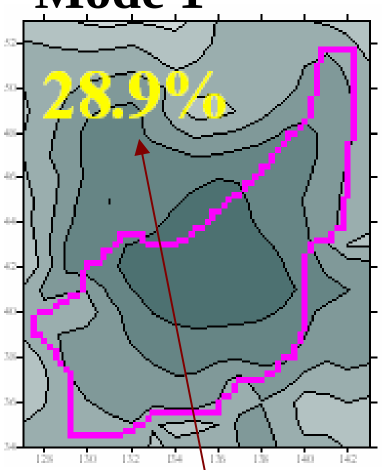

Leading complex EOF mode from wind vectors accounted for the general wind direction → effect of the East Asia monsoon (Trusenkova et al., 2009).

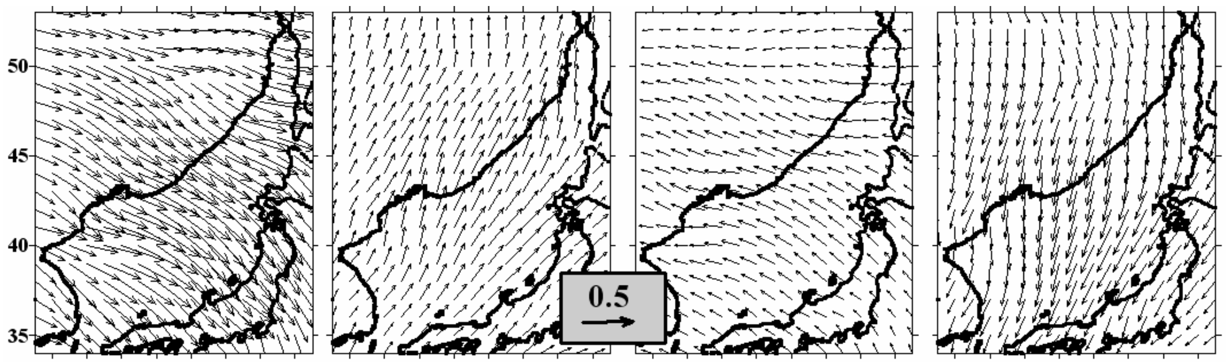

However,
fraction of the total variance was not high → any impact of higher modes?
There were fictional alongshore wind gradient zones → fictional curl zones.

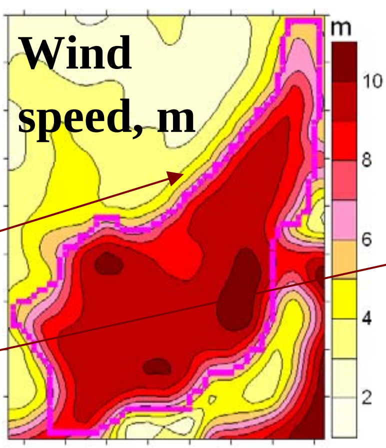

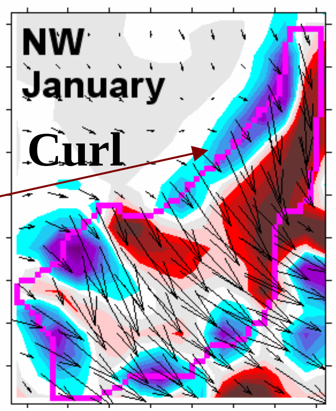

Purpose

To revisit the spatial/temporal patterns of wind stress and curl over the JES by multivariate statistical analysis of satellite scatterometry data

Sea winds from QuikSCAT

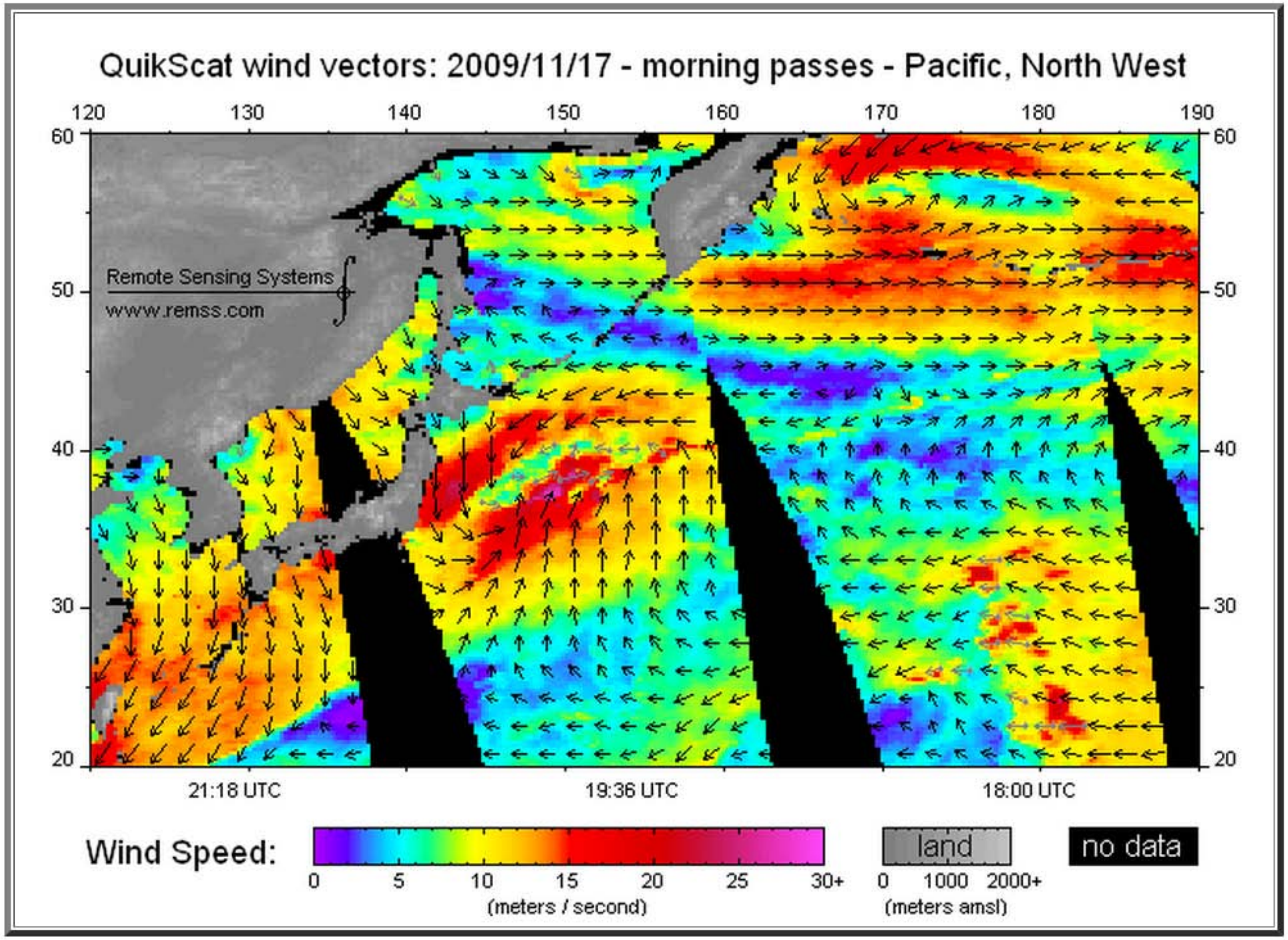

High resolution data over the water surface.

However, frequent gaps due to satellite swath divergence and rain contamination →

QSCAT merged with reanalysis provides data over the sea and land.

http://www.remss.com/qscat/scatterometer_data_daily

Data

QSCAT/NCEP Blended Ocean Winds

from Colorado Research Associates,

July 1999 - July 2009,

34°-53°N, 127°-143°E (JES and adjacent land),

6 hours, 0.5° grid,

1287 wind stress boxes and

386 stress curl boxes (over the sea only),

14724 times.

Techniques of EOF analysis

1) The complex form of the EOF analysis applied to wind vectors.

$X(r, t) = \sum A_k^*(r)B_k(t)$, where

$X(r, t) = U(r, t) + iV(r, t)$, U/V are zonal/meridional wind components,

$A_k(r) = \mathcal{A}_k(r)e^{-i\varphi}$ are spatial CEOFs and * denotes complex conjugate,

$B_k(t) = \mathcal{B}_k(t)e^{-i\phi}$ are principal components (PCs),

$\mathcal{A}_k$, $\mathcal{B}_k$ are spatial and temporal amplitudes ~ mode intensity,

φ_k, ϕ_k are spatial and temporal phases (-180°, 180°) ~ wind shear in space and time.

2) Correlations → detection of low amplitude signals ~ wind over the land

Covariances ~ signal magnitude → anomalies from weaker signals can be lost.

3) Low-pass filtering → by the inverse wavelet transform,

Morlet mother wavelet of the 6th order.

Decompositions of wind stress vectors

- Original dataset.
- Low-pass filtered dataset, with the 7- and 15-day cut-off periods.

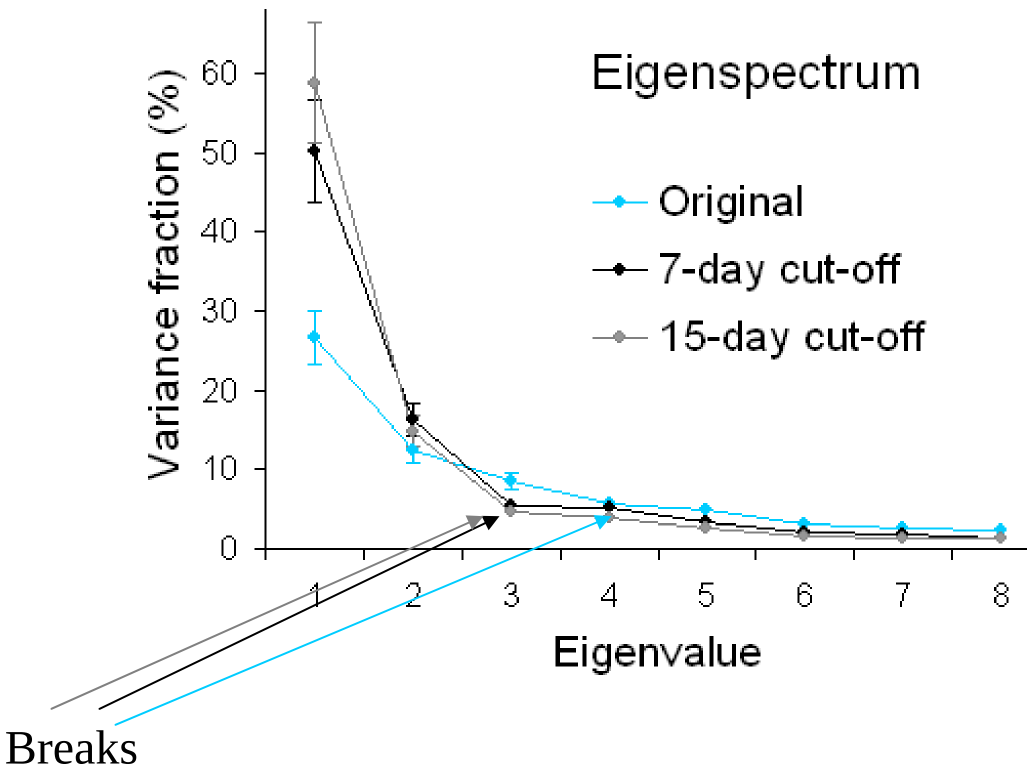

Modes 1 – 3
from the original data
and
modes 1 & 2
from the filtered data
pass the Montecarlo test
and are non-degenerate in the sense of errors.

High fraction of variance (>50%) for mode 1 from the filtered data.

Similar variance fraction for mode 2.

CEOF modes of wind stress vectors: spatial patterns

Similar patterns of modes 1 & 2 from the original and filtered data.

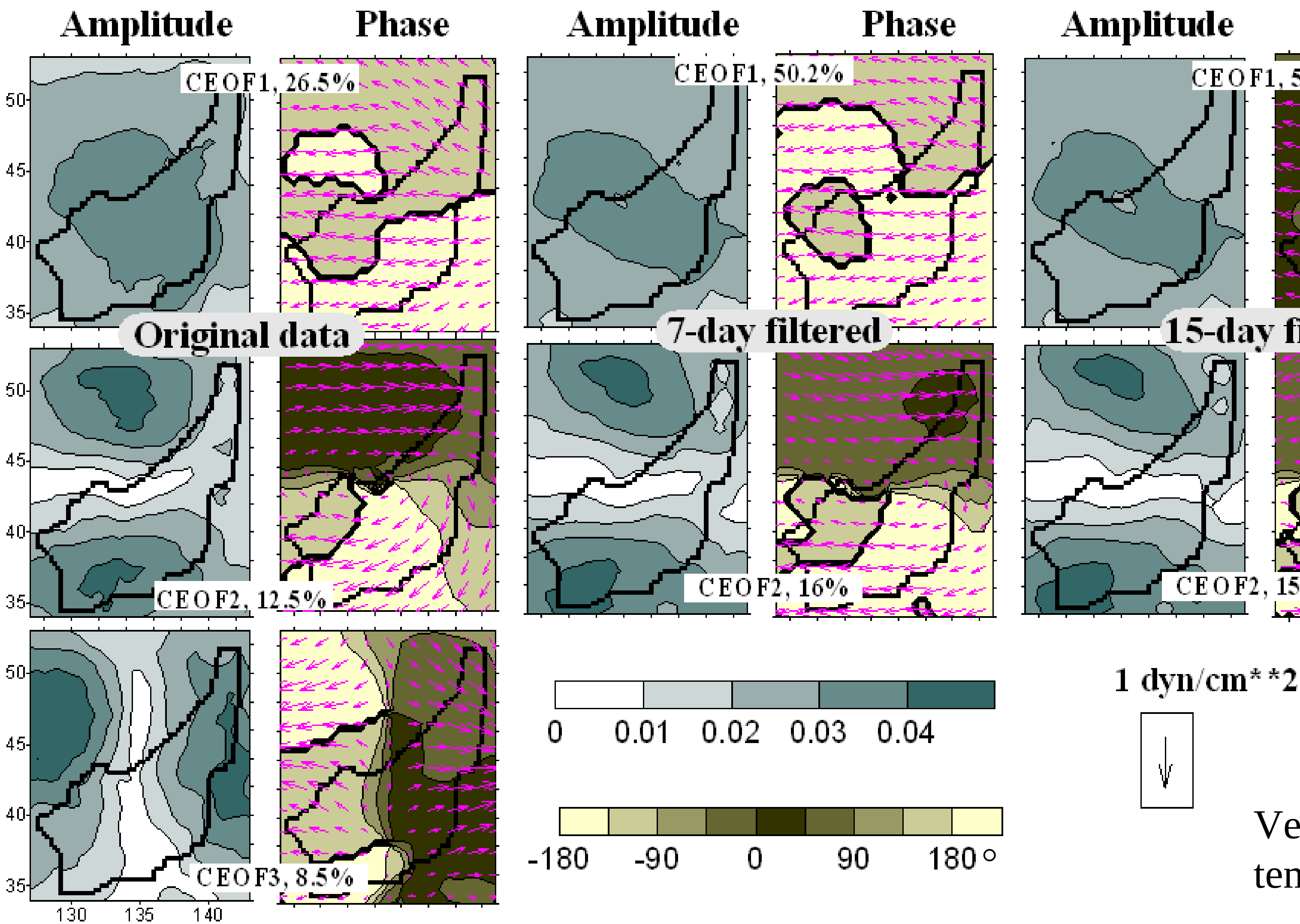

Vectors for zero temporal phase

CEOF modes of wind stress vectors: temporal patterns

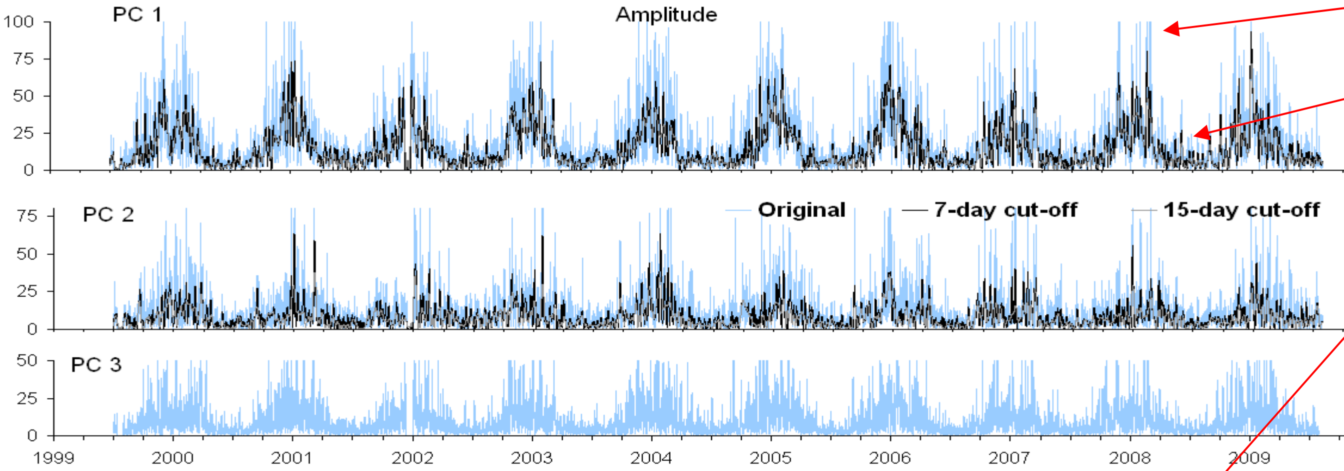

Winter:
strong wind
Summer:
weak wind

Winter:
Persistent NW wind
Summer:
changeable wind

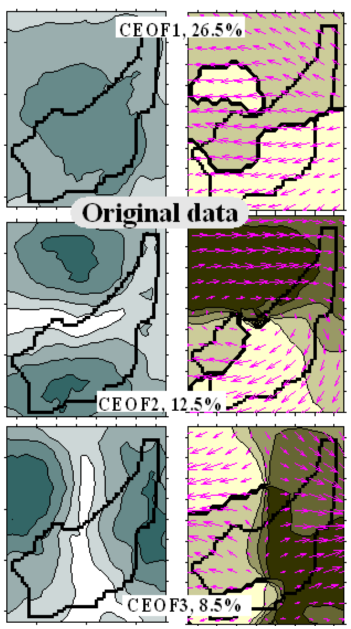

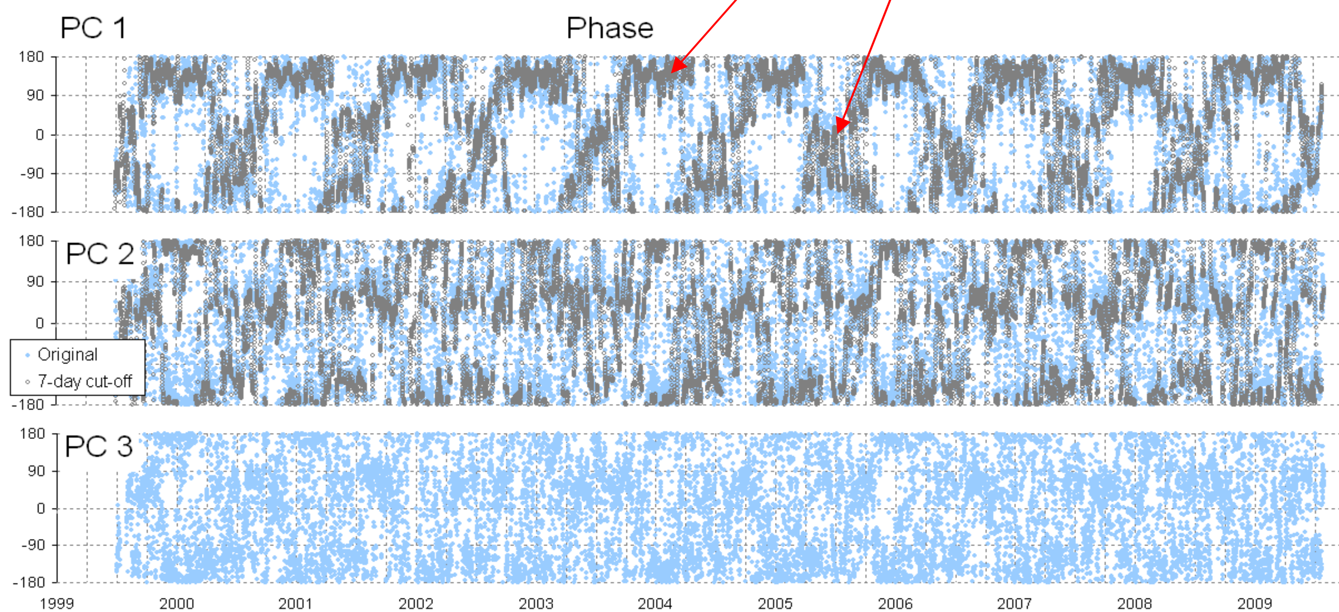

Mode 1: general wind direction

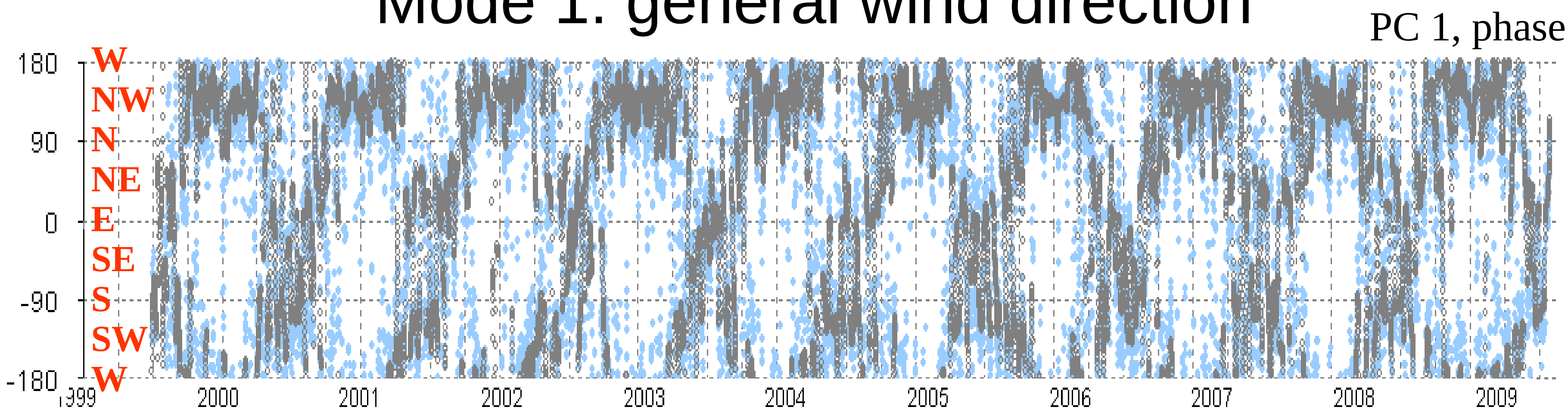

$X_k(r,t)=(A_k\,(r)e^{-i\varphi(r)})^* B_k(t)^{e-i\phi(t)}$

$\phi_t=0°$ ~ eastern wind

$\phi_1=135°$ ~ NW wind

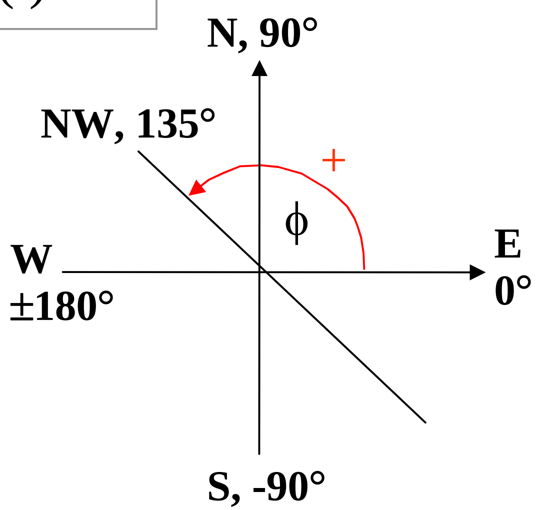

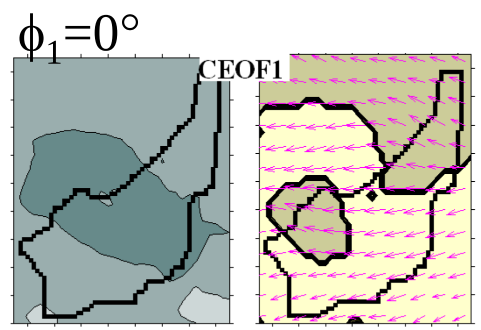

Noisy original $\phi(t)$, patterns of seasonal wind shifts in the filtered data.

Mode 2:
wind seesaw over the southern and northern JES

PC 2, phase

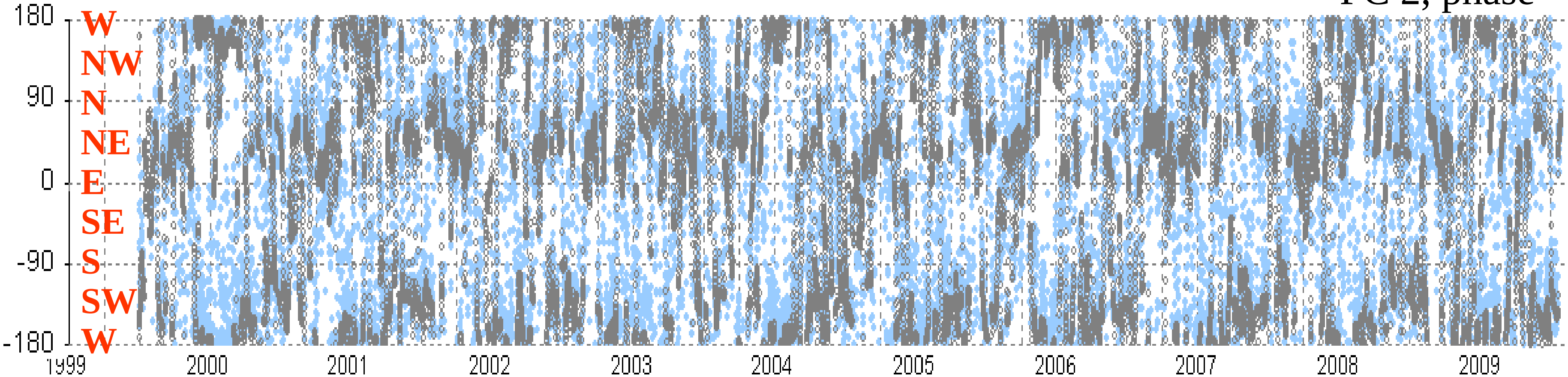

ϕ = 0 ~ eastern wind

Typical contribution of mode 2 from the filtered data set

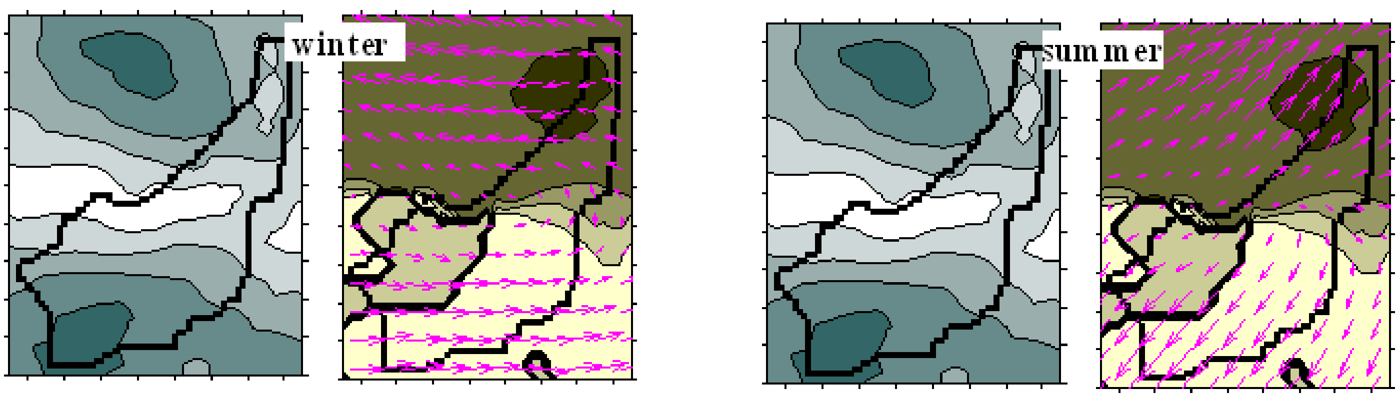

Mode 3: cyclonic / anticyclonic vortex
(original fields only)

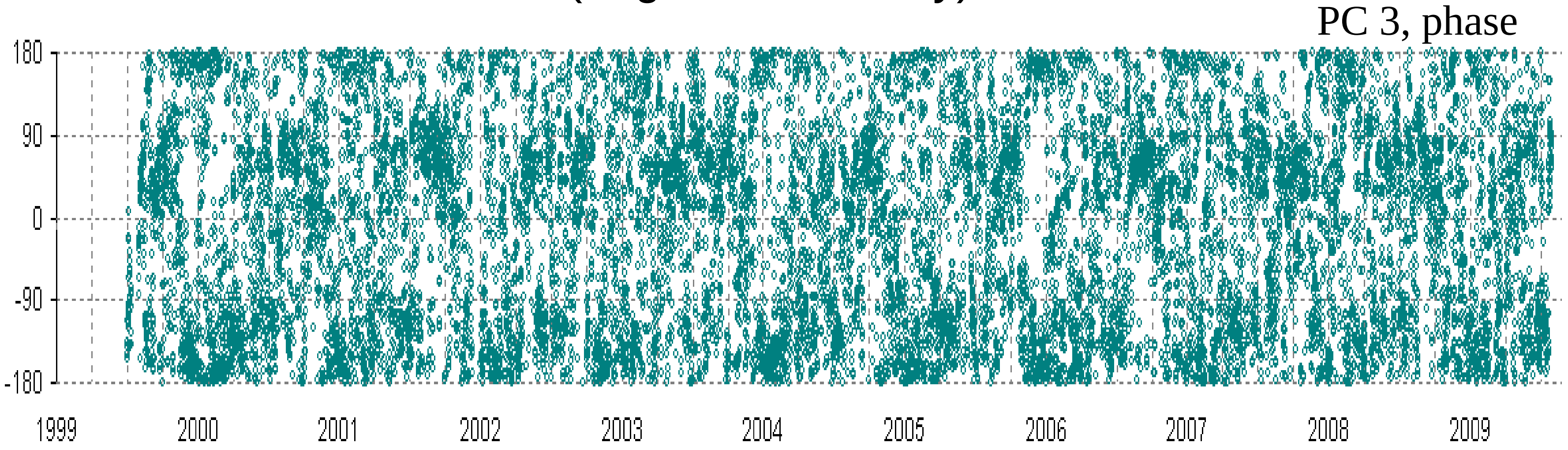

Typical contribution of mode 3

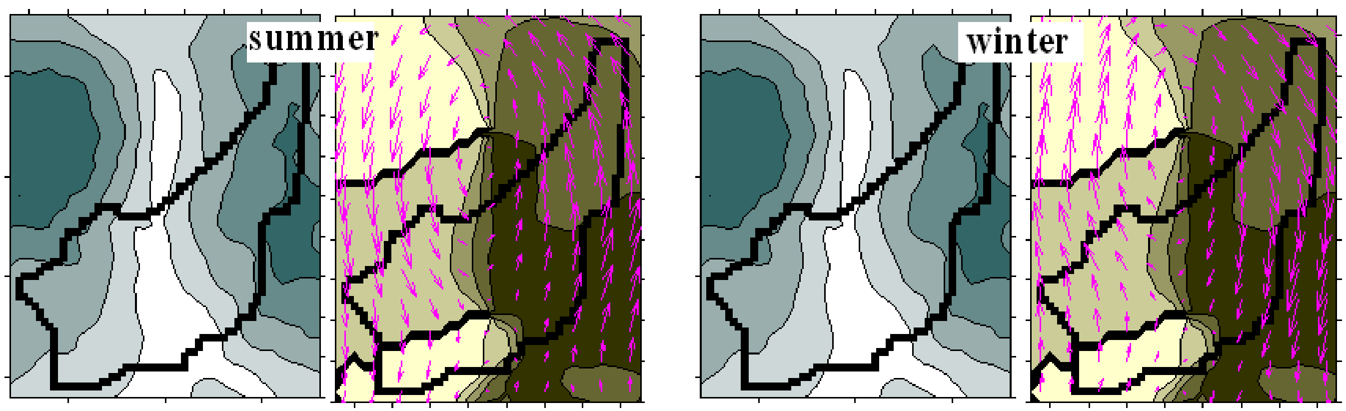

Cyclone Anticyclone

General wind direction:
any contribution from the higher modes?

Wind shift due to CEOF 2

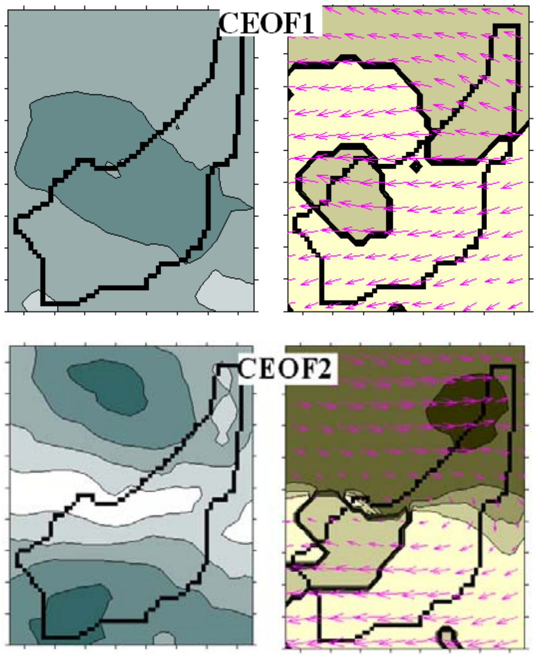

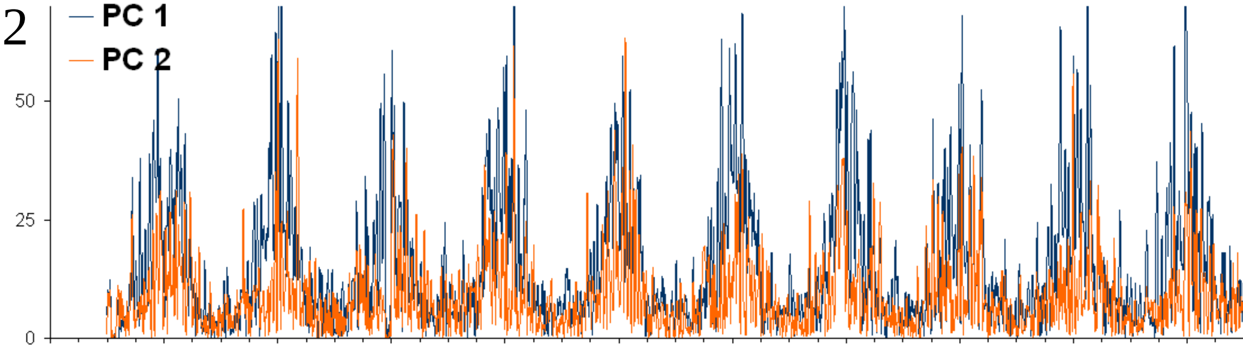

Temporal amplitude: PC1/PC2=1.5.

Wind shift:
< 10° in the northern JES
and <20° off the Tsushima Strait

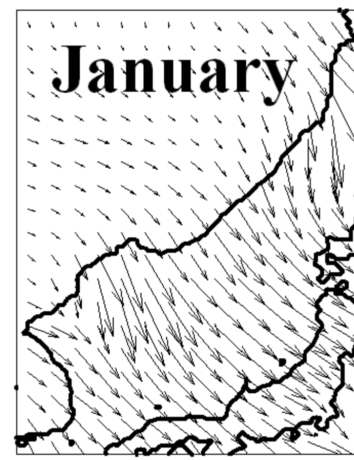

Mode 3 does not affect the wind shifts beyond the synoptic scale

---

General wind directions over the JES can be deduced from the leading mode alone –

The East Asia Monsoon Mode

Monthly occurrence of the monsoon winds

(from the temporal phase of mode 1 from low-pass filtered data)

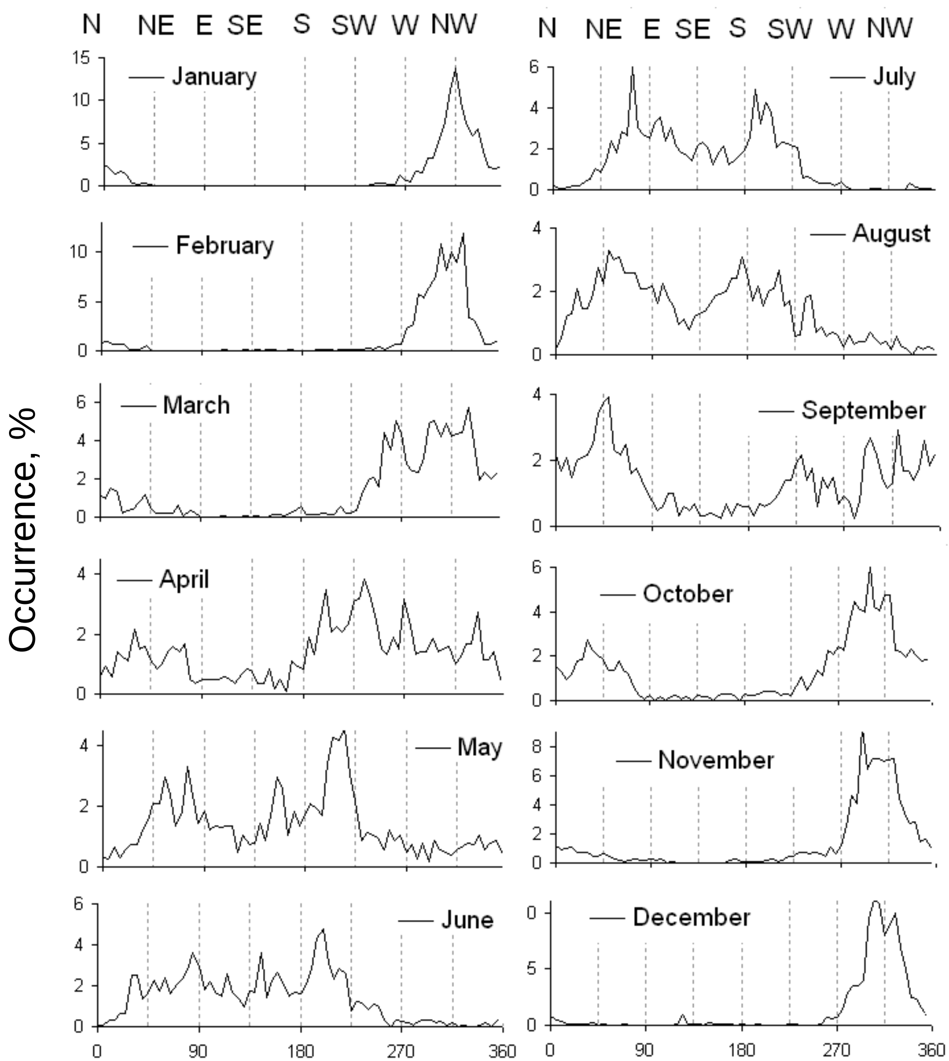

5°-gradation histograms

Phase transform

$$\phi' = -\phi + 90°$$

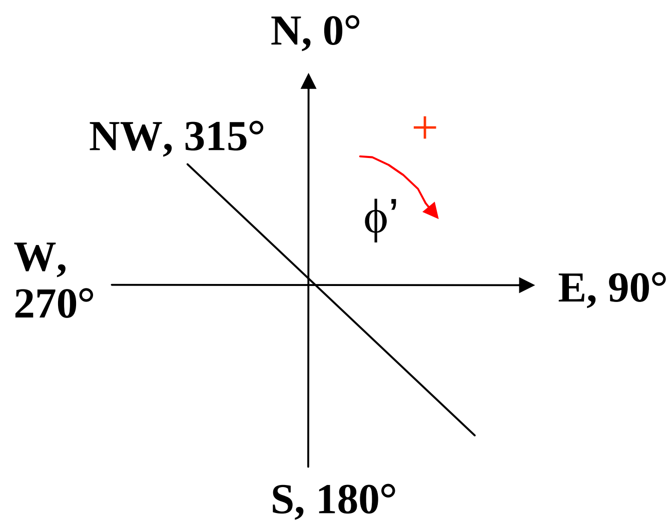

$\phi'=0°$ ~ northern wind

$\phi'=315°$ ~ NW wind

Monthly occurrence of the monsoon winds

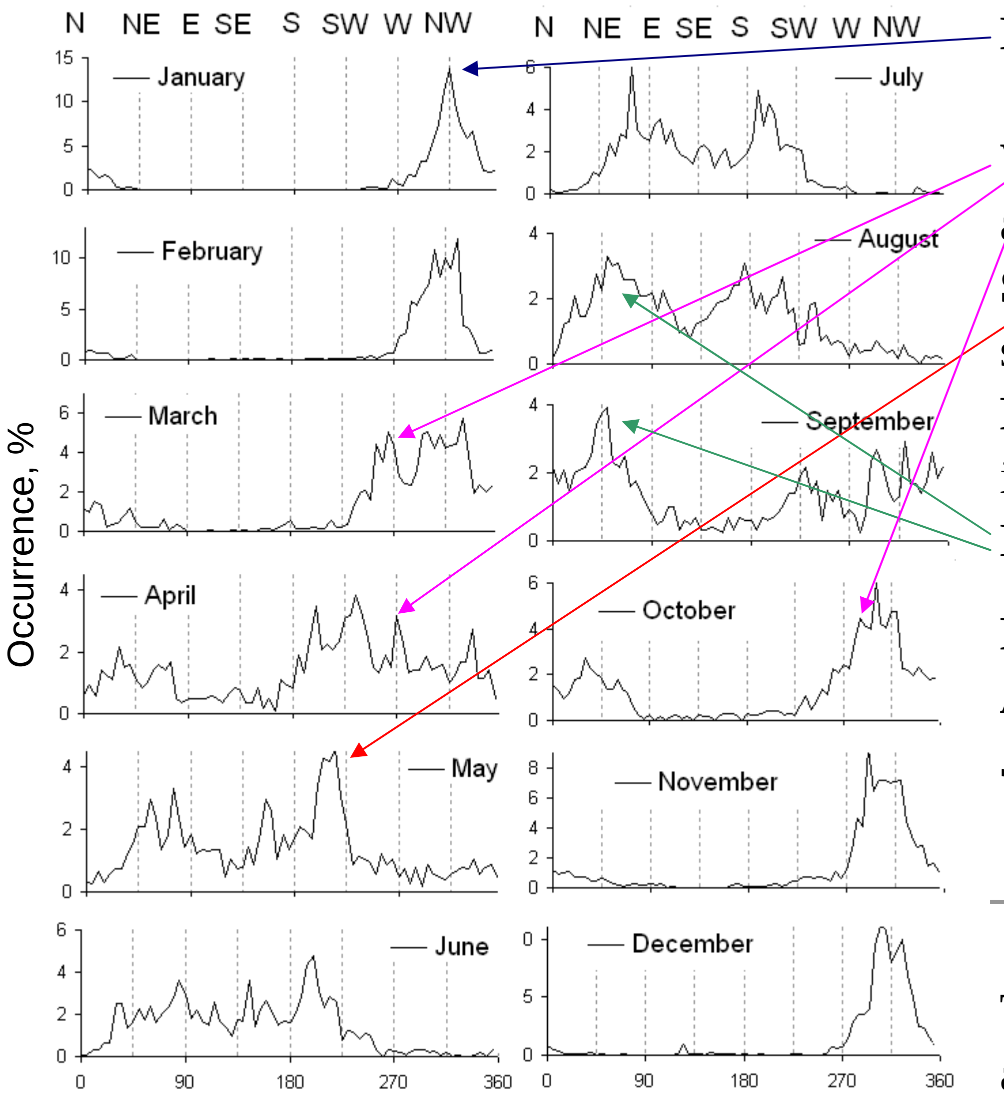

5°-gradation histograms

NW: dominant in November through February;
W: separate mode in March and April and merged with NW in October;
SW: occurs in April through September, strongest in May and June;
Easterly modes: occur more frequently in late summer;
NE: strong in August and September.

November – February: the only mode;
April and September: fuzzy;
July: bimodal (SW and E).

The southern wind is never a dominant mode.

Seasonal wind shifts

PC 1, phase

Winter

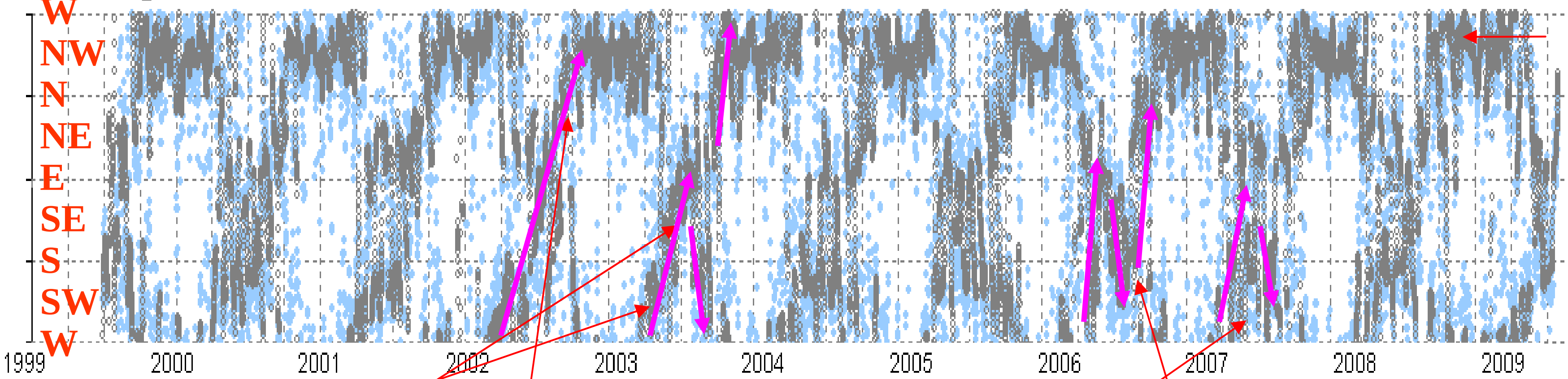

Prevailing transitions:

Spring: NW → W → SW

Summer: SW → SE → E

Autumn: E → NE → N → NW or E → SE → SW → W → NW

Strong intraseasonal shifts beyond the synoptic time scale

Time series of monsoon winds
(beyond the synoptic time scale)

$$X_1(t) = (A_1^{av} e^{-i\varphi 1av})^* B_1 e^{-i\phi 1}(t)$$

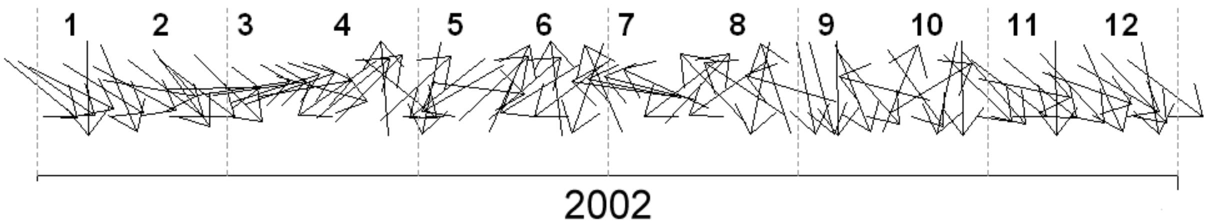

Autumn: E → NE → N → NW

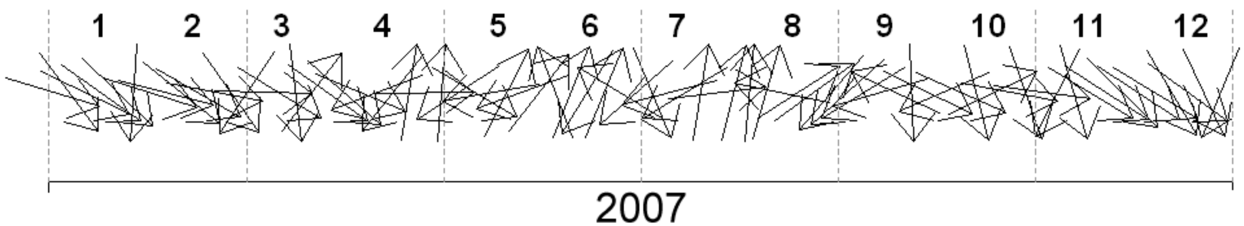

Autumn: E → SE → SW → W → NW

Intraseasonal variability beyond the synoptic scale (1 vector for 5 days shown)

Typical patterns of wind stress and curl

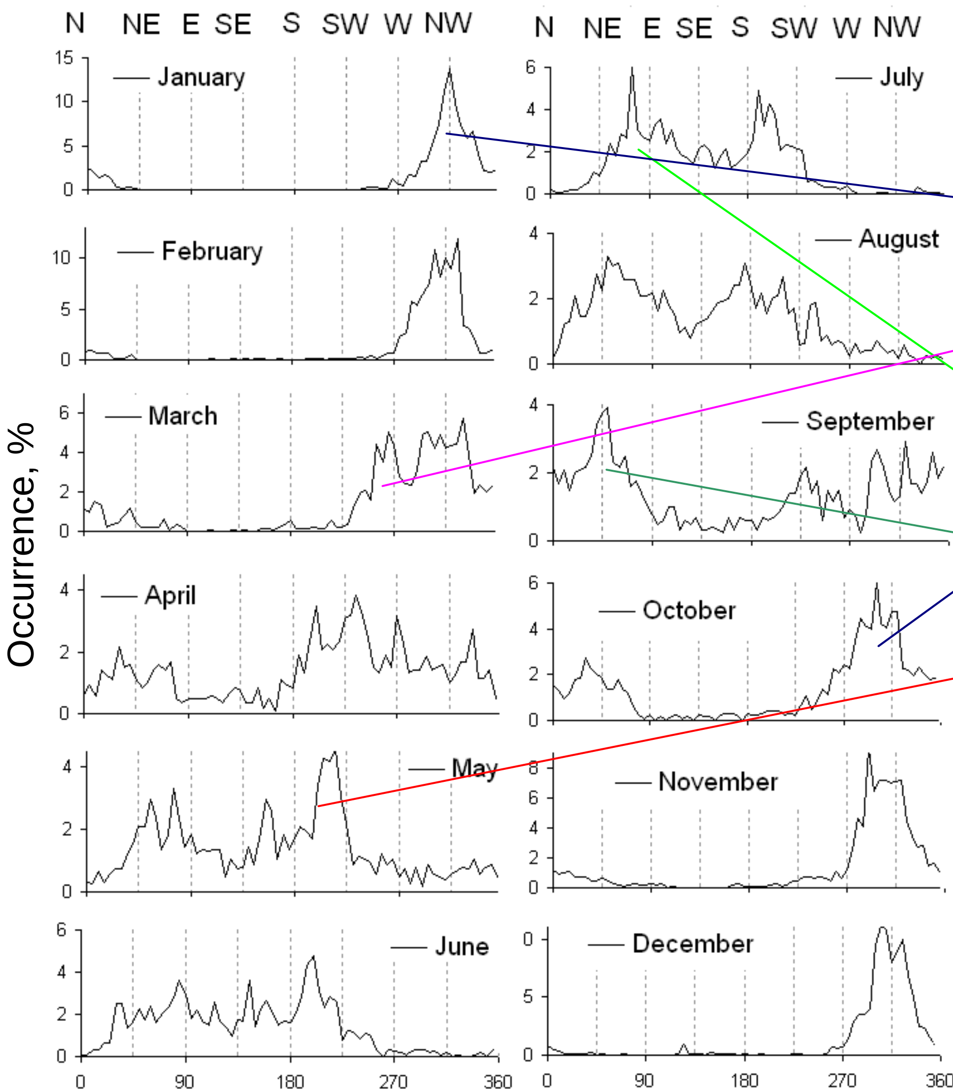

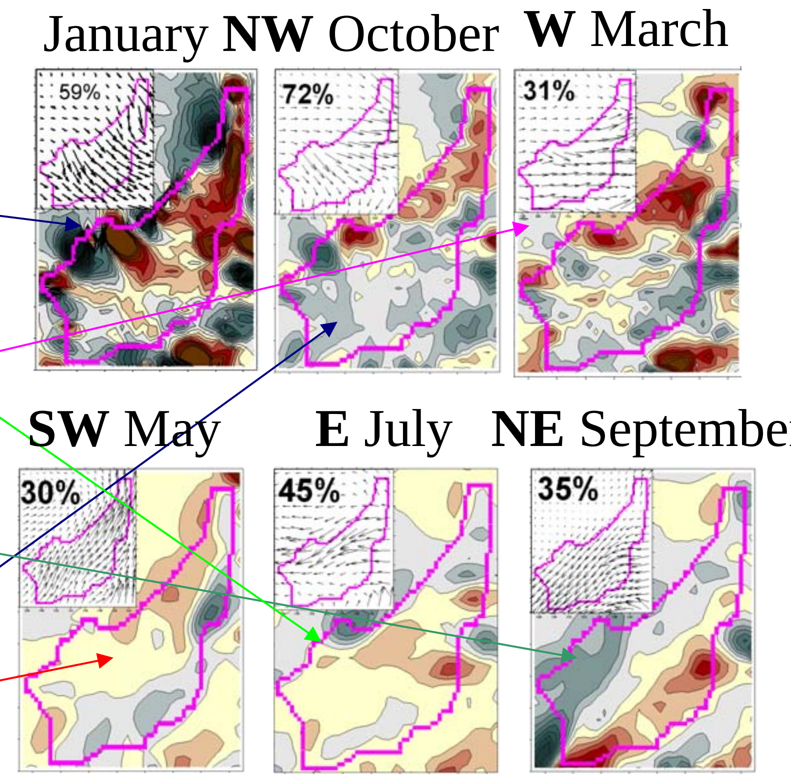

Stresses averaged within histogram modes; curls computed from the average stresses.

Stresses from April through October smoothed with 3-point window.

Decomposition of wind stress curl

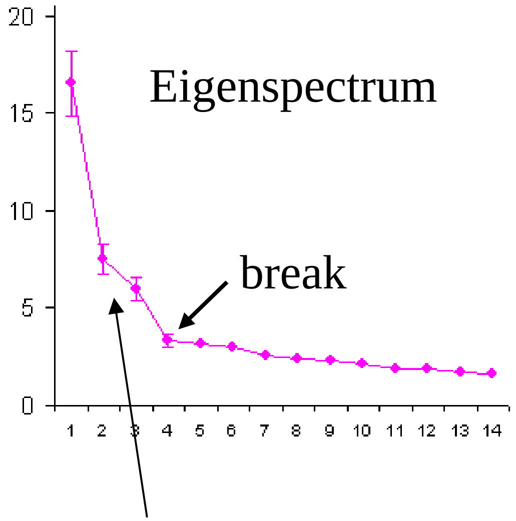

EV 2 and 3 are close, followed by a break

Low-pass filtered wind stress curl fields, with the 40-day cut-off period.

Modes 1-3 are statistically significant

Mode 1 can be considered separately

Modes 2 and 3 are better considered together

EOF modes of low-pass filtered wind stress curl

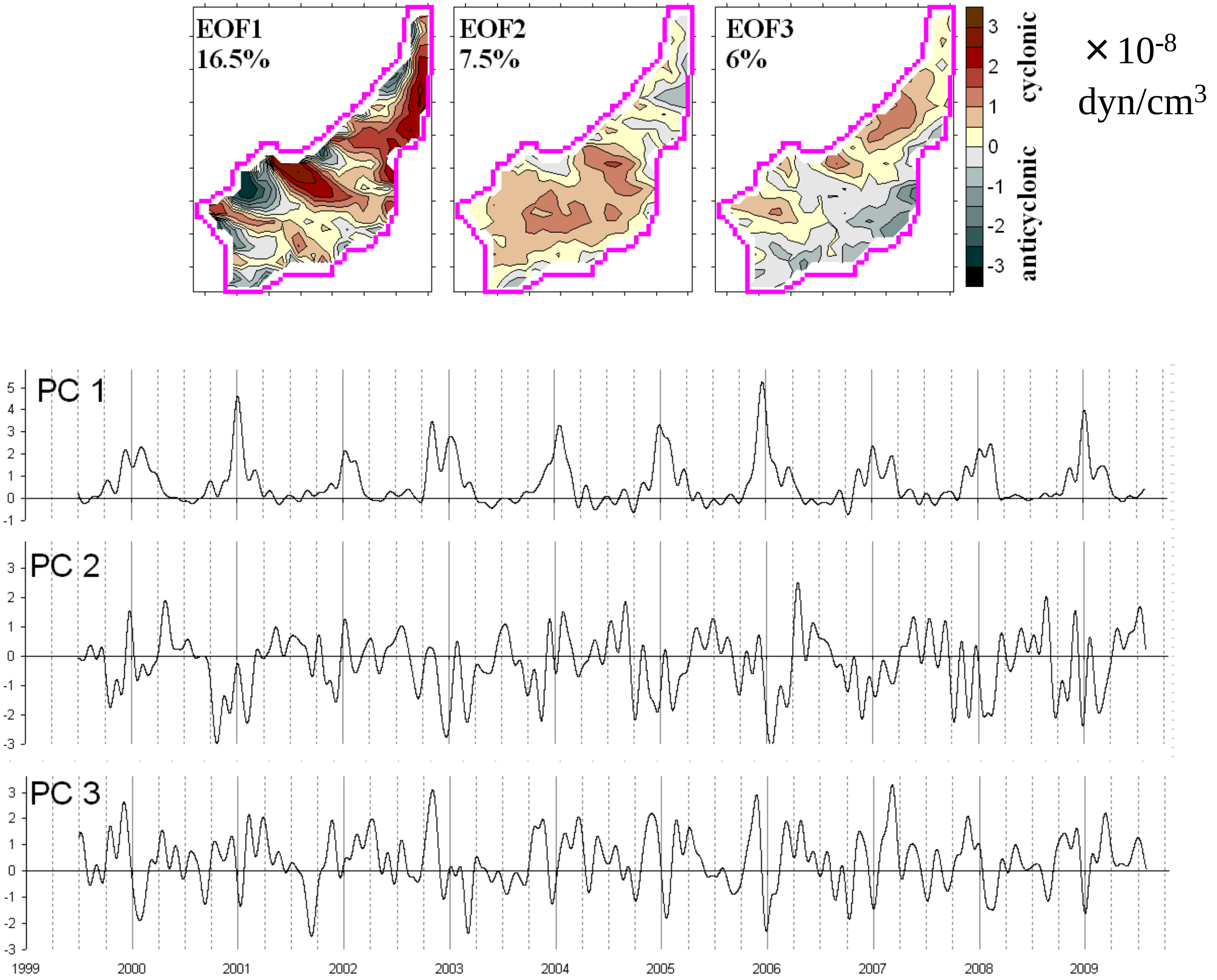

Winter mode

Topographic gaps

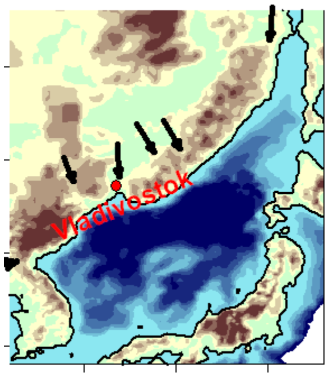

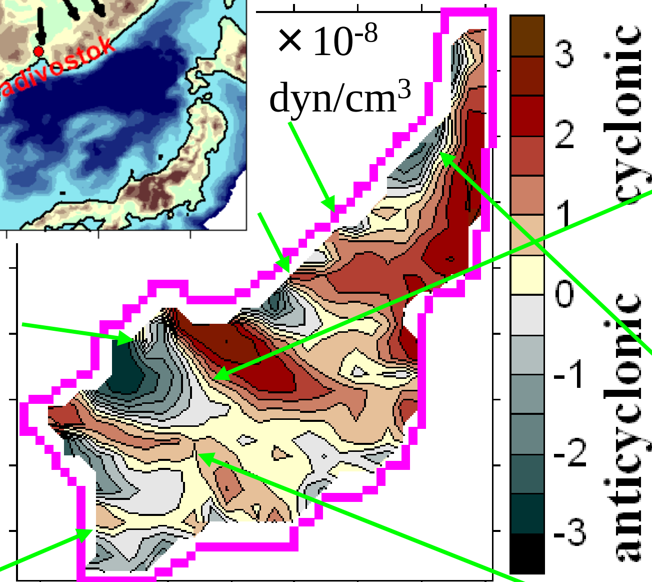

The EKWC separation from the coast

Cyclonic curl;
curl dipole
off Vladivostok
(Kawamura and
Wu, 1998),
several dipoles near
the western coast,
AC curl zone off
Khabarovsky Krai
coast,
cyclonic curl zone
off the
East Korea Bay.

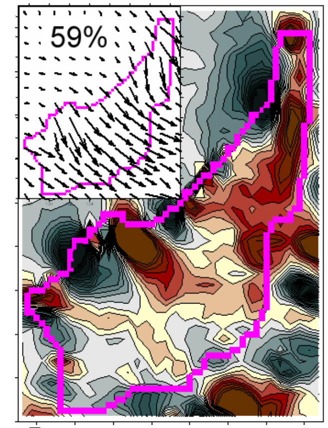

January, stress
from histogram

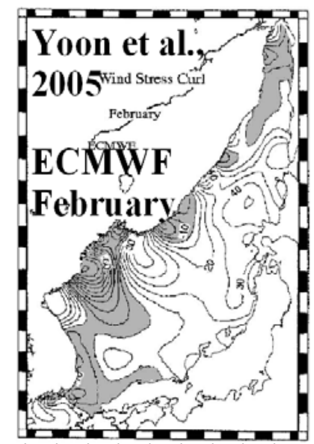

Strong mode:
winters 2000/2001,
2005/2006

Weak mode:
winters 2001/2002
2006/2007,
2007/2008

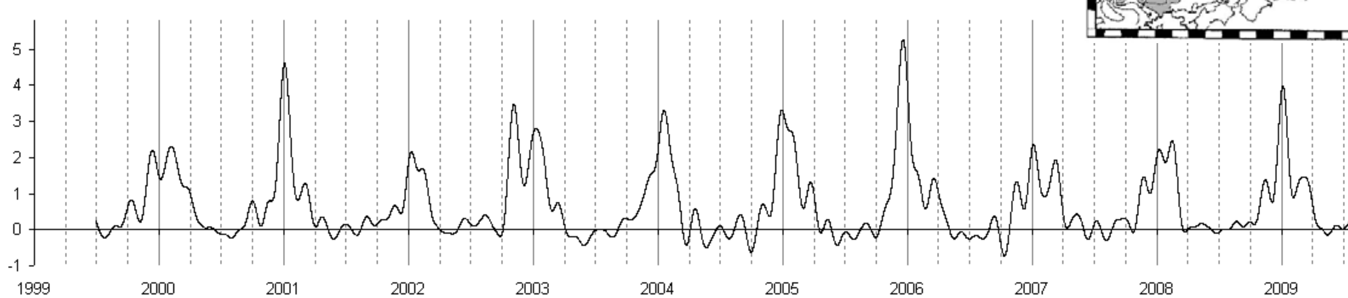

PC1 is above zero in November through February (mid March)

Warm season mode: combined effect of EOF 2 and EOF 3

(significant when PC 1 is close to zero)

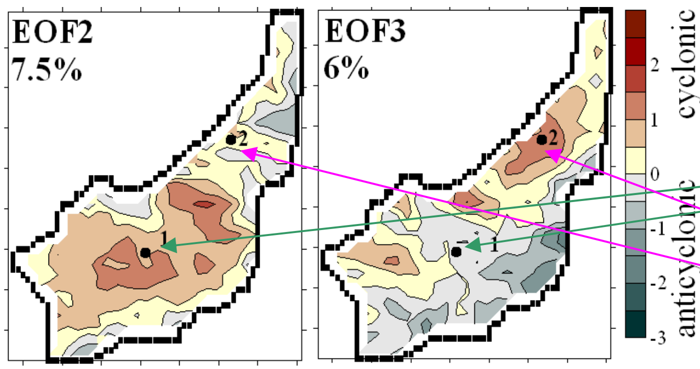

Strong southward of 43°N

Strong northward of 43°N

Contribution of modes 2 and 3

$X_{1,2}(t) = A_2(r_{1,2})B_2(t) + A_3(r_{1,2})B_3(t)$

Box 1 (central JES): EOF 2 dominates, corr(PC2, X_1) = 0.98

Box 2 (northeastern JES): EOF 3 dominates, corr(PC3, X_2) = 0.97

Curl ($\times 10^{-8}$ dyn/cm^3)

Warm season mode: the central JES

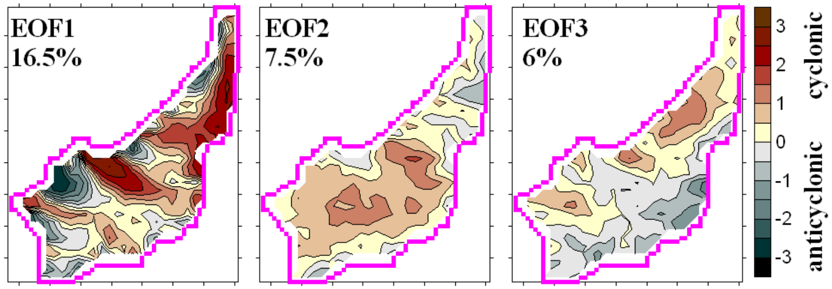

AC curl in late winter and autumn, oscillating between cyclonic and zero (slight AC) curl in late summer.

NW wind in March and October: AC curl

July

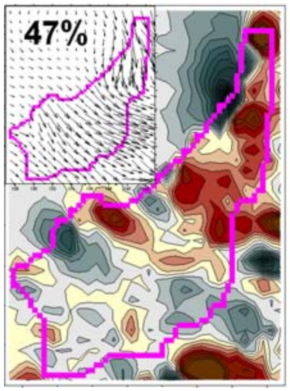

March

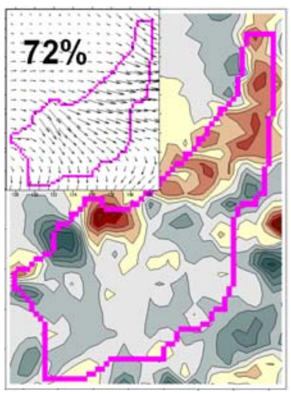

October

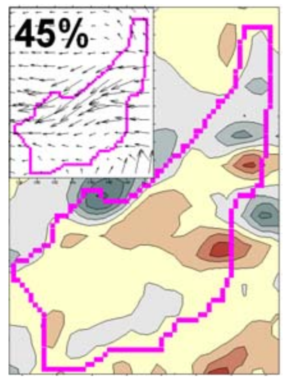

Eastern wind, frequent in late summer

April 2000, 2006: strong cyclonic curl.

Curl (× 10^{-8} dyn/cm^3)

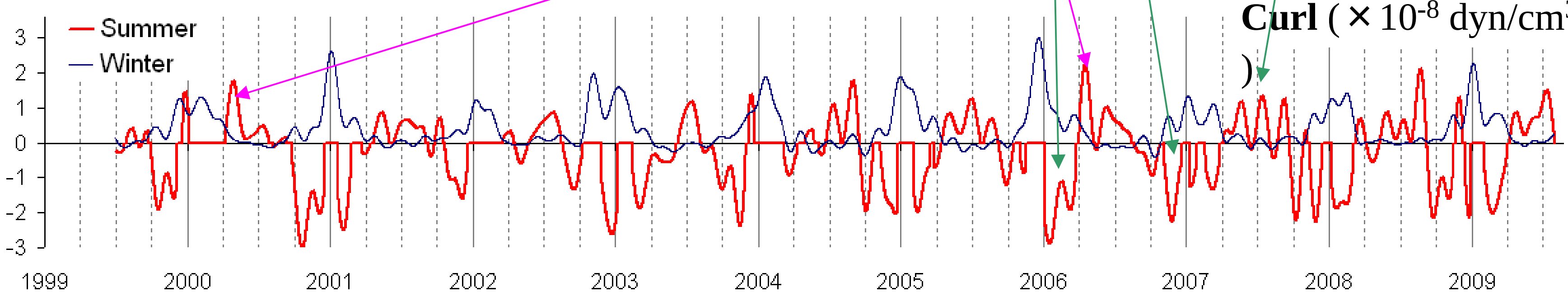

Winter/summer curls for the median spatial EOFs; summer curl when exceeds the winter curl

Warm season mode: the northeastern JES

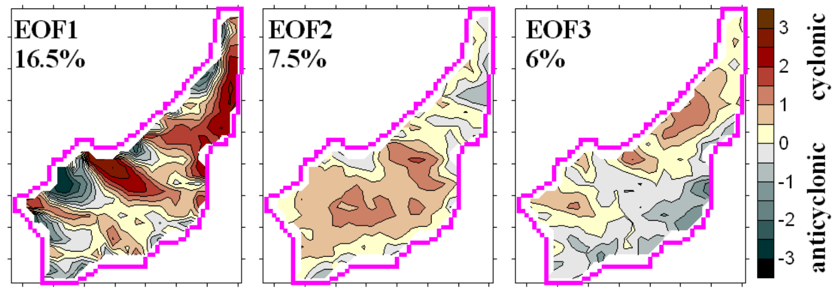

April

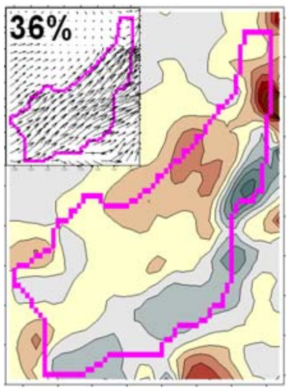

Western or SW wind, frequent in spring and autumn

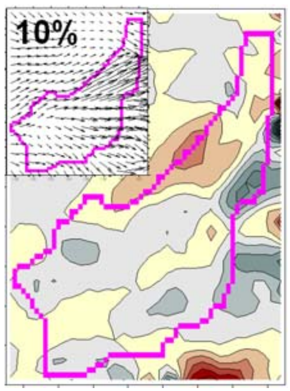

April

October

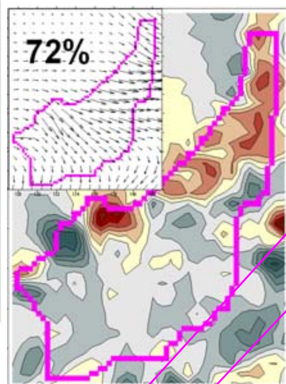

Cyclonic curl in spring/early summer and autumn, frequent AC curl in late summer.

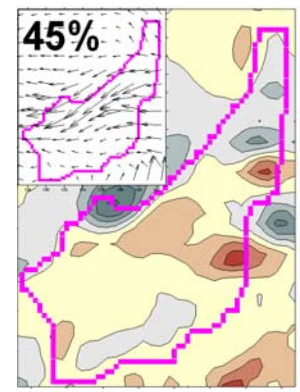

July

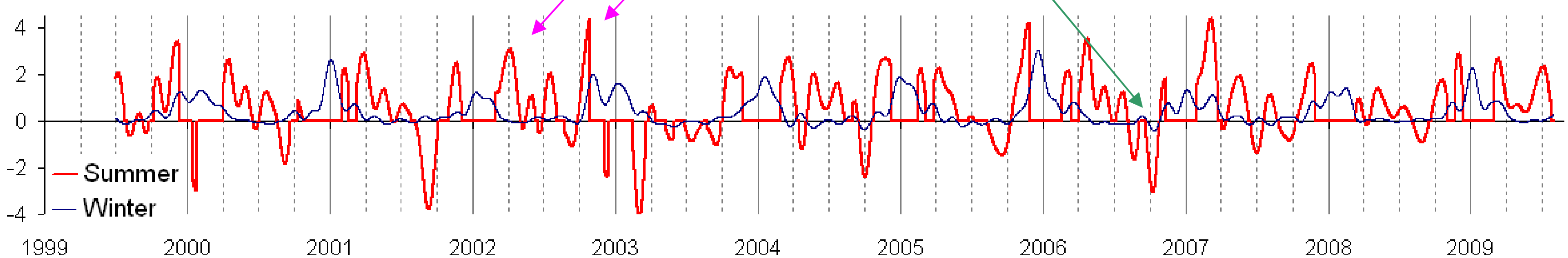

Winter/summer curls for the median spatial EOFs; summer curl when exceeds the winter curl

Conclusion

• The East Asia Monsoon pattern with characteristic wind directions and seasonal shifts is the leading complex EOF mode of wind stress over the JES.

•Contribution of higher modes is not significant.

•The results are consistent with the previous findings from reanalysis data (Trusenkova et al., 2009).

•Winter pattern is the leading EOF mode of wind stress curl. Fine features are resolved, such as several curl dipoles related to orographic gaps.

•Over the central JES, the AC wind stress curl prevails in late winter and autumn, while oscillations between the cyclonic and weak AC curl occur in summer.

•Over the northeastern JES cyclonic curl prevails in spring and autumn.